Implications of pannexin 1 and pannexin 3 for keratinocyte differentiation

Steven J. Celetti[1], Kyle N. Cowan[2], Silvia Penuela[3], Qing Shao[3], Jared Churko[3] and Dale W. Laird[1,3,*]

[1]Department of Physiology and Pharmacology, University of Western Ontario, London, ON Canada, N6A 5C1
[2]Department of Surgery, University of Western Ontario, London, ON Canada, N6A 5C1
[3]Department of Anatomy and Cell Biology, University of Western Ontario, London, ON Canada, N6A 5C1
*Author for correspondence (dale.laird@schulich.uwo.ca)

Accepted 18 January 2010
Journal of Cell Science 123, 1363-1372

doi:10.1242/jcs.056093

Summary

Pannexin (Panx) 1 and Panx3 are integral membrane proteins that share some sequence homology with the innexin family of invertebrate gap junctions. They are expressed in mammalian skin. Pannexins have been reported to form functional mechanosensitive single-membrane channels, but their importance in regulating cellular function is poorly understood. In this study, Panx1 and Panx3 were detected in the epidermis of 13.5 day embryonic mice. Compared with newborn mice, there was less Panx1 expression in both thin and thick murine skin, whereas Panx3 expression was unchanged. To investigate the role of pannexins in keratinocyte differentiation, we employed rat epidermal keratinocytes (REKs) that have the capacity to differentiate into organotypic epidermis, and engineered them to overexpress Panx1, Panx1-GFP or Panx3. The expression of Panx1 or Panx3 resulted in the increased ability of REKs to take up dye, suggesting that cell-surface channels were formed. Compared with monolayer REKs, endogenous Panx1 levels remained unchanged, whereas the 70 kDa immunoreactive species of Panx3 was greatly increased in the organotypic epidermis. In monolayer cultures, ectopic Panx1 and Panx1-GFP localized to the plasma membrane, whereas Panx3 displayed both intracellular and plasma-membrane profiles. Although both pannexins reduced cell proliferation, only Panx1 disrupted the architecture of the organotypic epidermis and markedly dysregulated cytokeratin 14 expression and localization. Furthermore, ectopic expression of only Panx1 reduced the vital layer thickness of the organotypic epidermis. In summary, Panx1 and Panx3 are coexpressed in the mammalian epidermis, and the regulation of Panx1 plays a key role in keratinocyte differentiation.

Key words: Pannexins, Differentiation, Epidermis, Proliferation

Introduction

A family of vertebrate proteins termed pannexins is homologous in sequence to invertebrate innexins. Thus, they were originally proposed to have functions similar to both innexin and connexin gap junctions (Panchin et al., 2000). Three pannexin (Panx) family members, Panx1, Panx2 and Panx3, have been identified in humans, rats and mice, but their functions within mammalian cells remain poorly understood (Baranova et al., 2004; Scemes et al., 2009). Panx1 transcripts are ubiquitously expressed in normal rodent and human tissues, and appear to be enriched in the central nervous system (Baranova et al., 2004; Iglesias et al., 2009; Penuela et al., 2007). Recently, the Panx1 glycoprotein was detected in several murine tissues, including the brain, spleen, cartilage and skin (Penuela et al., 2007). Two immunoreactive species of Panx3 – at ~43 kDa and 70 kDa – were found to be expressed in the skin, cartilage and heart (Penuela et al., 2007). Overall, although our understanding of the diverse localization patterns of the pannexins is beginning to unfold, the cellular role(s) of pannexins remain relatively obscure.

Despite the controversy surrounding whether pannexins form intercellular channels, reports continue to support the crucial role of pannexins acting as single-membrane channels in cellular communication with the extracellular environment (Scemes et al., 2009). Panx1 has been shown to be able to oligomerize into hexameric structures that traffic to the cell surface (Boassa et al., 2007) to form cell-surface membrane channels that can be blocked by pharmacological reagents (Bruzzone et al., 2005). Upon mechanical stress, Panx1 single-membrane channels have been implicated in the release of ATP, resulting in Ca^{2+} wave propagation through ATP-induced purinergic receptor activation (Bao et al., 2004). Additionally, Panx1 has been reported to respond to high extracellular K^+ levels and is associated with $P2X_7$ nuclear receptor ($P2X_7R$)-mediated activation of the caspase-1 cascade involved in neural inflammasome activation (Silverman et al., 2009). Although much less is known about the channel capabilities of Panx3, both Panx1 and Panx3 are glycoproteins capable of dye uptake, supporting their role as functional single-membrane channels (Penuela et al., 2007; Penuela et al., 2009).

As pannexins continue to be better understood as single-membrane channels, distinct subcellular and tissue-expression profiles of endogenous and ectopically expressed Panx1 and Panx3 are beginning to emerge. Earlier, we demonstrated that exogenously expressed Panx1 and Panx3 localized predominantly to the cell surface in normal rat kidney and BICR-M1R_K cell lines, and formed functional single-membrane channels capable of dye uptake upon overexpression in 293T cells (Penuela et al., 2007; Penuela et al., 2009; Penuela et al., 2008). Tissue-specific localization of endogenous Panx1 includes post-synaptic sites in cortical and hippocampal neurons, suggesting a potential role in regulating neuronal post-synaptic activity (Zoidl et al., 2007). In MDCK cells, endogenous Panx1 and Panx3 were localized to the cell surface (Boassa et al., 2007; Penuela et al., 2008), whereas Panx1 was found to be uniformly distributed throughout the cytoplasm in cells of the mouse spleen (Penuela et al., 2007). Similarly, in human facial skin

Journal of Cell Science

keratinocytes, Panx1 and Panx3 were found predominantly at cell-surface and intracellular locations, respectively, suggesting that these pannexins might have distinct roles in skin differentiation, maintenance or regeneration (Penuela et al., 2007). Although punctate Panx1 localization was detected chiefly in the stratum granulosum and spinosum layers of human facial epidermis, Panx3 expression exhibited a more scattered distribution throughout all epidermal layers and seemed to have a cytoplasmic subcellular distribution (Penuela et al., 2007). Together, the distinct cellular and subcellular localization profiles of Panx1 and Panx3 provide evidence to suggest that the spatio-temporal expression of pannexins in the skin might have implications in fundamental keratinocyte processes.

In this study, we hypothesize that the differential expression and localization of Panx1 and Panx3 in the skin are exquisitely regulated and play a key role in the differentiation, proliferation and/or maintenance of the epidermis. To that end, we characterized the expression of Panx1 and Panx3 in mouse epidermis under steady-state conditions and also assessed their role in rat epidermal keratinocyte (REK) differentiation into the organotypic epidermis.

Results

Differential Panx1 and Panx3 localization and expression levels in murine skin

The integrity of mouse tissue sections was first evaluated by hematoxylin and eosin (H&E) staining of newborn skin, three-week-old thin skin (dorsal), three-week-old thick skin (paw) and skin containing sebaceous glands (Fig. 1A). Immunofluorescent labeling revealed that Panx1 was localized to intracellular compartments of suprabasal layer cells of newborn skin and throughout all vital layers of epidermal thin skin (Fig. 1B). By contrast, Panx1 expression was below detectable levels in thick skin and sebaceous glands (Fig. 1B). Panx3, on the other hand, exhibited diffuse intracellular localization throughout all vital epidermal layers of thin skin, most notably in the basal layer and keratin-expressing sebocytes (Fig. 1D). Unlike Panx1, a diffuse intracellular staining profile of Panx3 was revealed in all vital epidermal layers of thick skin, but was undetected in newborn skin. These results suggest that Panx1 and Panx3 might play diverse roles in murine skin, temporally and spatially. To ensure that all immune staining was specific, a peptide pre-adsorption assay was used to block anti-pannexin antibody binding (Fig. 1C,E).

To assess the expression of Panx1 and Panx3, skin samples were subjected to immunoblotting. Because Panx1 is extensively glycosylated (~41-48 kDa), it resolves as multiple bands within a western blot (Penuela et al., 2007). Panx1 levels were reduced in three-week-old thin and thick murine skin compared with newborn skin (Fig. 2A,B). On the other hand, Panx3 levels were similar in newborn and three-week-old skin, which included both the ~43 kDa and 70 kDa immunoreactive species (Fig. 2C,D). To ensure that the anti-pannexin antibodies were both specific and recognized multiple Panx1 and Panx3 species, REKs were engineered to overexpress either Panx1 or Panx3 prior to immunoblotting for both pannexins in the presence or absence of cognate peptide used to generate the antibodies (Fig. 2A). These results support the notion that Panx1, but not Panx3, might be temporally regulated in the epidermis. To assess the differentiation state of the epidermis, we examined the expression levels of two molecular markers of epidermis differentiation, cytokeratin 14 (CK14) and involucrin. Somewhat expectedly, involucrin, but not CK14, had increased expression levels in thick skin compared with newborn skin (Fig. 2E,F). In all cases, GAPDH was used as a housekeeping loading control.

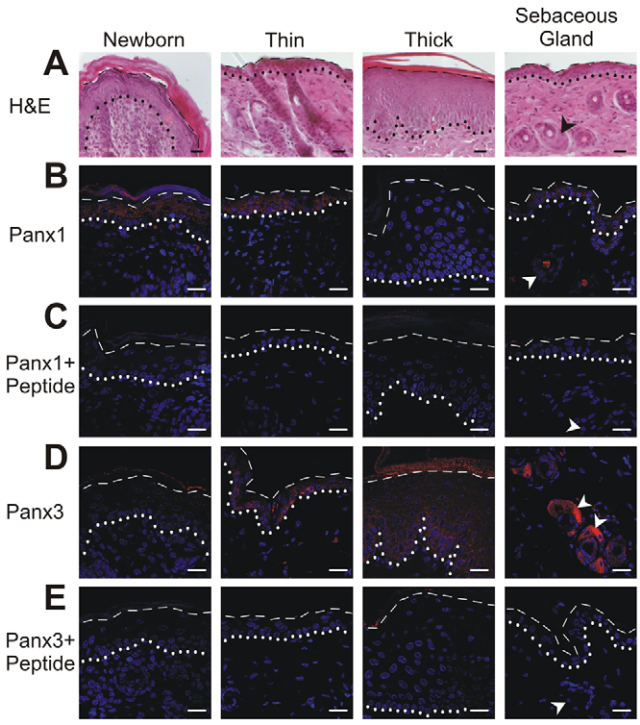

Fig. 1. Panx1 and Panx3 are differentially expressed within murine skin. (**A**) Images of murine skin biopsies stained with H&E reveal the epidermal architecture of newborn skin and the thin and thick epidermis of three-week-old mice. The basal layer is located above the dotted line and the cornified layer is above the dashed line. An image of a sebaceous gland (arrowhead) next to a hair follicle was obtained from the dorsal area of a three-week-old mouse. Tissue sections were stained with either (**B**) anti-Panx1 or (**D**) anti-Panx3 antibodies or the same antibodies in the presence of their respective cognate peptides (**C**,**E**), and counterstained with Hoechst (blue). Staining profiles revealed intracellular Panx1 (B; red) localization in the suprabasal layer of newborn skin and throughout all layers of thin epidermis. By contrast, Panx1 was not detectable in thick skin and barely detectable in sebaceous glands. On the other hand, Panx3 (D) was detectable in all thin and thick epidermal layers, but favored an intracellular localization profile in the basal layer and sebaceous glands (arrowheads) of thin skin. In contrast to Panx1, Panx3 was barely detectable in newborn skin. Scale bars: 20 μm.

To determine the onset of Panx1 and Panx3 expression in the CK14-positive developing epidermis, we assessed the expression and localization of these pannexins in the epidermis of embryonic day (E)13.5 mice. Interestingly, both Panx1 and Panx3 were readily detected in the epidermis and within the underlying cells (Fig. 3). Competition assays with cognate peptides revealed that the majority of the Panx1 and Panx3 immunostaining was specific (Fig. 3).

Localization of ectopically expressed Panx1 and Panx3 in REKs

REKs that did not express detectable levels of pannexins (Fig. 4A) were engineered to express Panx1 or Panx3. When REKs expressed Panx1 or Panx1-GFP, they predominantly localized to the cell surface (Fig. 4B; green), with little colocalization with the endoplasmic reticulum (ER)-resident protein protein disulfide

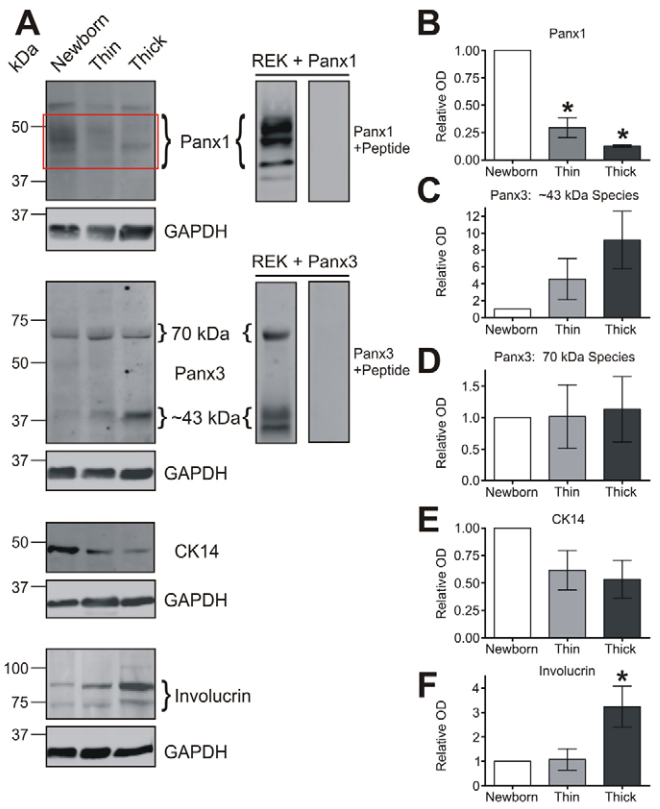

Fig. 2. Panx1, but not Panx3, expression levels decrease in aging and thickened murine skin compared with newborn skin. (**A**) Western blots of Panx1, Panx3, CK14 and involucrin from newborn, thin and thick skin. The specificity of the anti-Panx1 and anti-Panx3 labeling was assessed by immunoblotting REKs overexpressing Panx1 or Panx3 in the presence and absence of cognate peptides used to generate the antibodies. GAPDH was used as a loading control and the red box denotes the glycosylated species of Panx1. Less Panx1 expression was detected in three-week-old thin and thick skin compared with newborn skin (**B**), whereas the expression levels of both the ~43 kDa and ~70 kDa immunoreactive species of Panx3 remained relatively unchanged (**C**,**D**). Although the ~43 kDa species appeared to increase in thick skin, this was not statistically significant, perhaps because of the dilution effect of non-epidermal tissue present in the lysate. CK14 exhibited no change in expression between the different mouse skin types (**E**); however, involucrin expression did increase in thick skin compared to newborn skin (**F**). Bar graphs represent relative optical densities (OD) to GAPDH and the newborn sample is normalized to 1 (± s.e.m.).

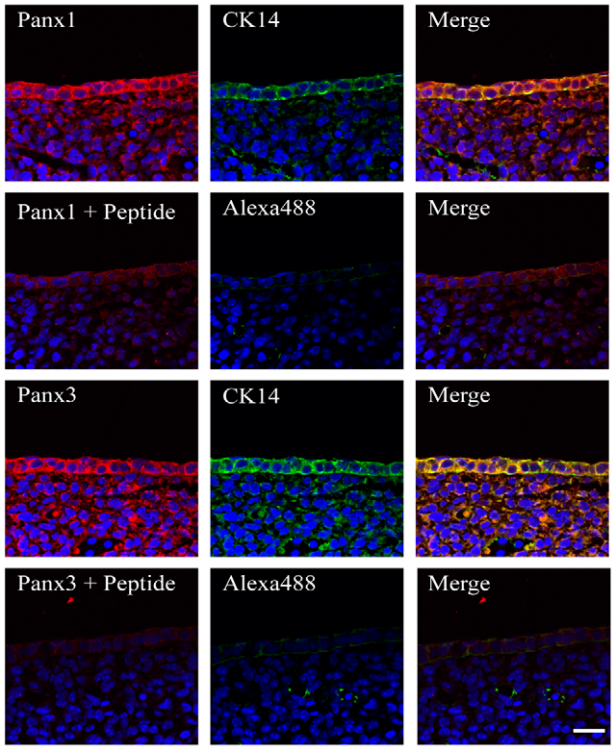

Fig. 3. Panx1 and Panx3 were detected in the epidermis of E13.5 mice. Paraffin sections of E13.5 mouse embryos were double immunolabeled for Panx1 or Panx3 (red) and CK14 (green). Note the presence of both pannexins in the CK14-positive epidermis. Anti-Panx1 and anti-Panx3 antibodies, along with their cognate peptides, were used to label sections on separate slides to account for any non-specific tissue labeling (left panels, rows 2 and 4; red). The controls for CK14 labeling consisted of the same sections where only the secondary antibody (Alexa488) was used (middle panels, rows 2 and 4; green). Scale bar: 50 μm.

isomerase (PDI) (Fig. 4B,C; red). On the other hand, Panx3 localized to the cell surface in an estimated 70% of the cell population (Fig. 4D; green), while exhibiting an intracellular colocalization pattern with PDI in ~30% of the cell population (Fig. 4E; yellow). These two localization profiles of Panx3 were observed randomly throughout the monolayer REK cultures. Specific anti-pannexin labeling was confirmed by peptide pre-adsorption assays (Fig. 4B,D; inserts).

REKs expressing pannexins are capable of dye uptake and exhibit decreased cell proliferation, whereas migration properties are unchanged

We have previously shown that 293T cells take up fluorescent dyes upon overexpression of Panx1 or Panx3 (Penuela et al., 2007). To ascertain whether REKs also take up dye upon pannexin overexpression, stable cells lines were mechanically stimulated and incubated with rhodamine (sulforhodamine B), and dye uptake was assessed (Fig. 5A). Sulforhodamine was readily visualized in Panx1-, Panx1–GFP- and Panx3-expressing cells, but was not observed in cells expressing the empty vector. The much larger dextran-rhodamine dye, used as a negative control, was not visualized in any of the cell lines (Fig. 5A). Because small dyes such as sulforhodamine can readily transfer among cells through connexin 43 (Cx43) gap junctions present in these cells (Langlois et al., 2007; Maher et al., 2005), the presence of dye reflects both dye uptake and intercellular dye transfer.

To further characterize pannexin-expressing REKs, we assessed the proliferative status of our REKs using a BrdU incorporation assay. Overexpression of Panx1, Panx1-GFP or Panx3 was found to decrease the percentage of BrdU-positive REKs by ~15-20% compared with both wild-type and empty vector controls (Fig. 5B). However, a cell-migration assay revealed that pannexin-expressing REKs migrated equally as well as controls over a 48-hour time period (Fig. 5C).

Panx1 expression is maintained in the organotypic epidermis

To assess the role of pannexins in REK differentiation, we employed a liquid-air chamber that induced the differentiation of wild-type

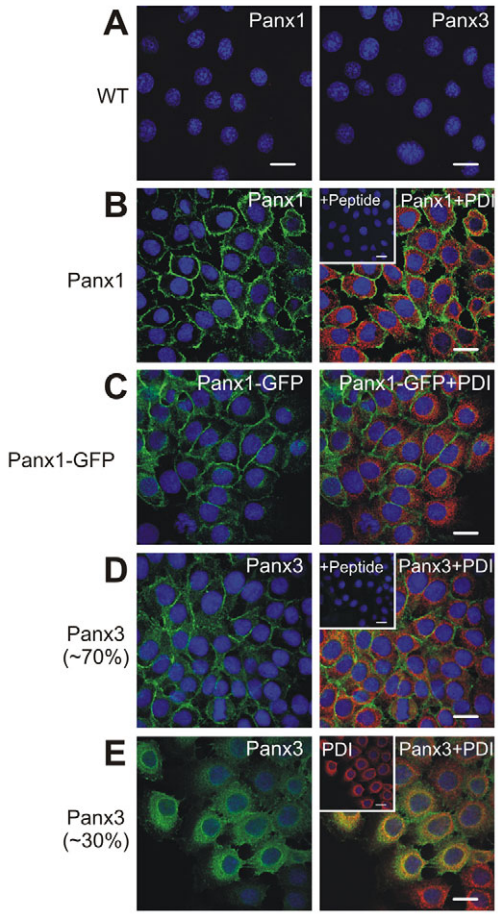

Fig. 4. Ectopically expressed Panx1 and Panx3 are predominantly localized to the cell surface in REKs. (**A**) Endogenous Panx1 and Panx3 were undetectable by immunocytochemistry in REKs. When overexpressed, Panx1 (**B**; green) and Panx1-GFP (**C**; green) were localized to the cell surface in REKs and did not colocalize with PDI (B,C; red). Similar to Panx1 and Panx1-GFP, ~70% of Panx3-overexpressing cells (**D**) localized Panx3 to the cell surface, whereas the remaining cells revealed an intracellular distribution pattern that colocalized with PDI (**E**, yellow). Peptide pre-adsorption assays eliminated Panx1 and Panx3 immunolabeling (B,D, inserts). PDI labeling only is shown in the insert in E; Hoechst nuclear stain is in blue. Scale bars: 20 μm.

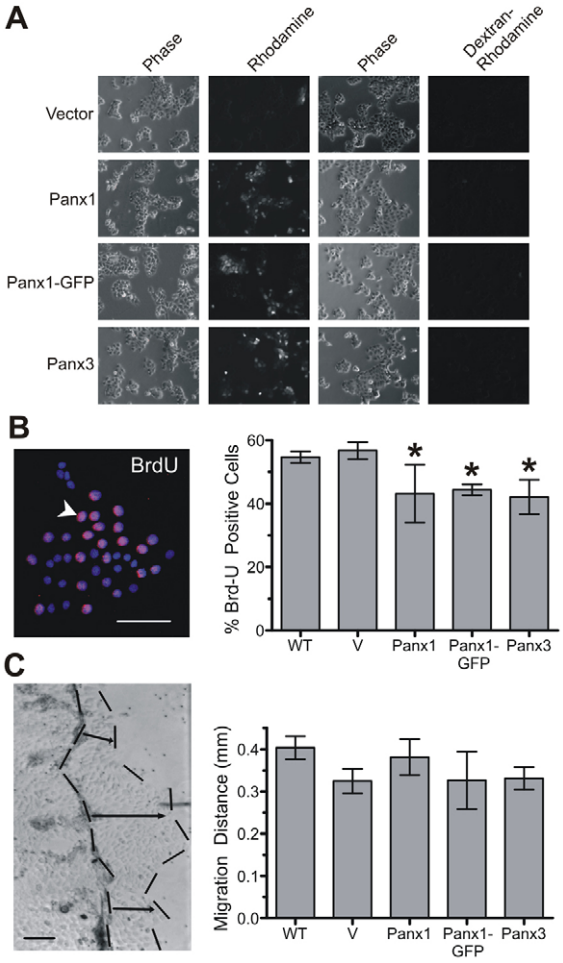

Fig. 5. Panx1- and Panx3-expressing keratinocytes are capable of dye uptake and exhibit reduced cell proliferation. (**A**) Stable REKs expressing Panx1, Panx1-GFP or Panx3 exhibited significant sulforhodamine B (rhodamine) dye uptake compared with vector-expressing controls, whereas there was no detectable dextran-rhodamine uptake in parallel experiments. Once dye uptake occurred, it would be expected to transfer to neighboring cells by means of Cx43 gap junctions. Cells were imaged under a 20× objective. (**B**) BrdU incorporation revealed that the proliferation rate of REKs overexpressing Panx1, Panx1-GFP or Panx3 was reduced. BrdU-positive nuclei (pink) were expressed as a percentage of total Hoechst-stained nuclei per viewing field. Asterisks denote statistical significance (n=5, P<0.05). (**C**) A scrape assay revealed that Panx1, Panx1-GFP or Panx3 did not influence the migration abilities of REKs after 48 hours (n=5, P>0.05). Scale bars: 100 μm B and 0.2 mm C. The bar graphs show means ± s.d. V, vector; WT, wild type.

REKs into a 3-5 cell thick vital layer and an overlying cornified layer (Fig. 6A). In monolayer cultures, multiple glycosylated species of endogenous Panx1 were only revealed in wild-type REKs when the blots were overexposed [Fig. 6B; WT (2) lane]. On the other hand, REKs exhibited increased expression of exogenously expressed Panx1 or Panx1-GFP when grown either in monolayer or as organotypic cultures, and the pannexin-labeling pattern could be competed with cognate peptide (Fig. 6B,C). Quantification of these data normalized to GAPDH revealed no significant difference in the expression levels of Panx1 in the organotypic epidermis and in monolayer culture.

The expression of the 70 kDa immunoreactive species of endogenous Panx3 increases when REKs are grown as organotypic epidermis

Low levels of the ~70 kDa immunoreactive species of endogenous Panx3 were detected by western blotting in monolayer REKs (Fig. 7A). The expression of this species greatly increased when cells were grown as organotypic epidermis, suggesting it might be important for keratinocyte differentiation (Fig. 7A,D). By contrast, the well-characterized doublet species of Panx3 at ~43 kDa exhibited no observable change in expression level in organotypic epidermis compared with monolayer cultures (Fig. 7A,C). When Panx3 was ectopically expressed in REKs, the doublet at ~43 kDa continued to be highly expressed when cells were grown in monolayers or as organotypic epidermis (Fig. 7A,C). To ensure that both the ~43 kDa and ~70 kDa immunoreactive species of Panx3 were bona fide Panx3 species, both species were eliminated when competed with cognate peptide (Fig. 7B). The ~70 kDa species of

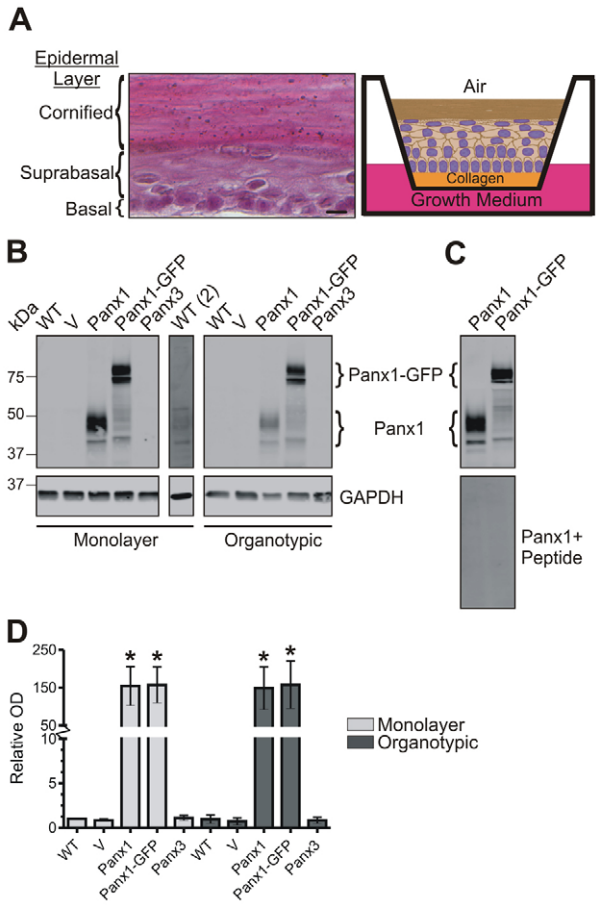

Fig. 6. Exogenous and endogenous expression of Panx1 in monolayer cultures and organotypic epidermis. (**A**) When grown on a collagen-coated filter and exposed to air, REKs differentiate into organotypic epidermis within 3 weeks, complete with 3-5 vital layers and a cornified layer. Scale bar: 10 µm. Western blotting (**B**) and subsequent densitometric quantification (**D**) revealed that overexpression of Panx1 (~41-48 kDa) and Panx1-GFP remained stable after multiple passages and when grown into organotypic epidermis. Wild-type REKs expressed low levels of Panx1, as revealed by overexposing the immunoblots [B; WT (2) lane]. GAPDH was used as a loading control and asterisks denote statistical significance (n=5, P<0.05). (**C**) Pre-adsorption of the anti-Panx1 antibody with its cognate peptide eliminated all antibody binding to Panx1 and Panx1-GFP. Bar graphs show normalized means ± s.e.m. V, vector; WT, wild type.

Panx3 was also detected with two additional antibodies raised against distinct Panx3 epitopes (data not shown).

Increased CK14 in Panx1-expressing organotypic REKs is suggestive of epidermal dysregulation

In parallel immunoblots, CK14 and involucrin expression levels were assessed as indices of keratinocyte differentiation. As would be expected for normal epidermis differentiation, in all cases, involucrin expression increased when REKs were grown into organotypic epidermis (Fig. 8A,C). Surprisingly, CK14 expression increased in Panx1-expressing organotypic epidermis compared with wild-type monolayer REKs, suggesting that differentiation was at least partially dysregulated in this case (Fig. 8B). The lack of a statistical significant change in Panx1-GFP upon CK14 expression might reflect reduced efficacy of Panx1 due to the GFP tag.

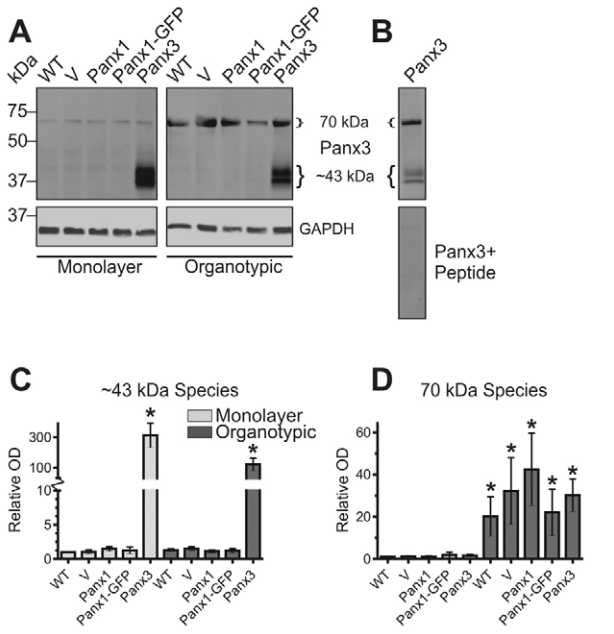

Fig. 7. Increased levels of the ~70 kDa immunoreactive species of Panx3 in organotypic epidermis. Western blotting (**A**) and subsequent densitometric quantification resulted in undetectable levels of the doublet Panx3 species at ~43 kDa (**C**) in wild-type REKs. GAPDH was used as a loading control and asterisks denote statistical significance compared with wild-type monolayer REKs (n=5, P<0.05). By contrast, endogenous levels of the ~70 kDa immunoreactive species of Panx3 (**D**) were significantly increased when REKs were allowed to differentiate into organotypic epidermis. Panx3 expression remained high when REKs were engineered to express Panx3 and grown in monolayer culture or as organotypic epidermis (A). (**B**) Pre-adsorption of the anti-Panx3 antibody with its cognate peptide eliminated specific antibody binding to both the ~43 kDa and ~70 kDa immunoreactive species. Bar graphs show normalized means ± s.e.m. V, vector; WT, wild type.

Panx1 expression dysregulates keratinocyte differentiation, whereas elevated Panx3 expression maintains epidermal architecture

Organotypic epidermis grown from REKs expressing Panx1, Panx1-GFP or Panx3 was stained with H&E to reveal the epidermal architecture (Fig. 9A). Wild-type, empty vector and Panx3-expressing organotypic models resembled newborn murine skin, displaying an organized basal layer, 3-5 suprabasal layers of differentiated keratinocytes and a thick cornified layer. On the other hand, Panx1- and Panx1–GFP-expressing organotypic epidermis appeared dysregulated and disorganized. Dark-purple-stained nuclei were typically identified as undifferentiated keratinocytes, suggesting that exogenous Panx1 might partially inhibit keratinocytes from entering the differentiation program. In addition to the dysregulation of keratinocyte differentiation by Panx1, Panx1 was found to significantly reduce the vital layer thickness (Fig. 9B). Although Panx1–GFP-expressing organotypic epidermis also appeared dysregulated, the vital layer thickness was similar to that of controls and the Panx3-expressing model. This suggests that the GFP tag on Panx1 might in fact partially alter the Panx1 function in keratinocytes.

Pannexins and cytokeratins are differentially localized in organotypic epidermis

In keeping with the weak Panx1 signal observed in western blots, Panx1 was not readily detectable by immunofluorescence in wild-

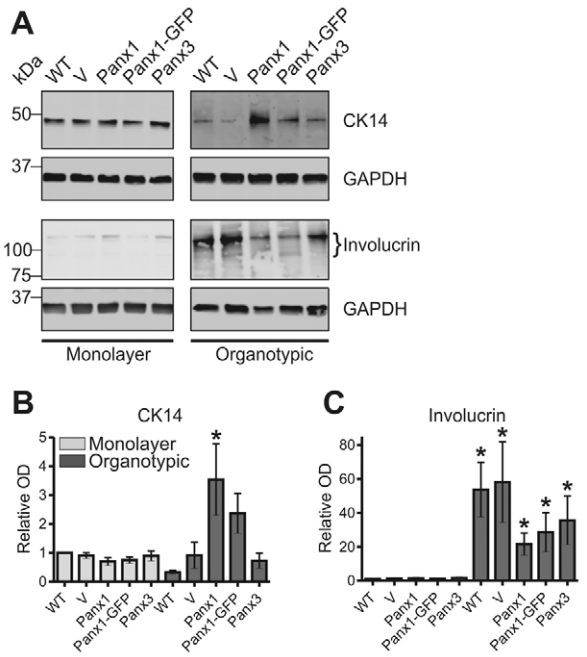

Fig. 8. An aberrant increase in CK14 in Panx1-expressing cells when grown as organotypic epidermis. (**A**) Western blotting revealed the levels of CK14 and involucrin in monolayer and organotypic epidermal models. GAPDH was used as a loading control. (**B**) Densitometric quantification revealed increased CK14 expression in Panx1-overexpressing organotypic epidermis. (**C**) Involucrin expression was increased in all organotypic cultures indicative of cell differentiation. Asterisks denote statistical significance (n=5, P<0.05) and bar graphs represent normalized means ± s.e.m. V, vector; WT, wild type.

type (not shown) or vector control organotypic epidermis (Fig. 10A). Surprisingly, Panx3 was only detected in the cornified layer of organotypic epidermis (Fig. 10A). As expected, CK14 was primarily localized to the basal layer, with weak evidence of its presence in suprabasal layers, whereas cytokeratin 10 (CK10), a marker of differentiated keratinocytes, localized mainly to the suprabasal layers. Consistent with the fact that ectopic pannexin expression is driven from the cytomegalovirus (CMV) promoter, we were not surprised to find that Panx1, Panx1-GFP and Panx3 were found in all keratinocyte strata, regardless of the state of cell differentiation (Fig. 10B-D). Interestingly, the pannexins (including Panx1-GFP) were observed more readily within intracellular compartments, as opposed to the cell surface, suggesting that they relocalized within the organotypic epidermis upon cell growth. Occasionally, Panx1 and Panx1-GFP were observed at the cell surface, suggesting that relocalization did not occur in at least some cells (Fig. 10B; arrowheads). Importantly, Panx1-expressing keratinocytes exhibited abnormal CK10 and CK14 localization patterns throughout all vital layers, providing additional evidence that REK differentiation is dysregulated when Panx1 is overexpressed (Fig. 10B). Although CK10 was predominantly localized to suprabasal layers in Panx1-GFP organotypic epidermis, CK10 was not consistently expressed in all suprabasal cells, as observed in vector controls. Whether cells expressed Panx1 or Panx1-GFP, CK14 was found throughout all epidermal layers, supporting the premise that Panx1, either untagged or tagged with GFP, perturbs keratinocyte differentiation (Fig. 10B,C). In cells expressing Panx3, CK10 localization appeared similar to that seen in vector controls, supporting the notion that Panx3 does not disrupt differentiation of REKs (Fig. 10D).

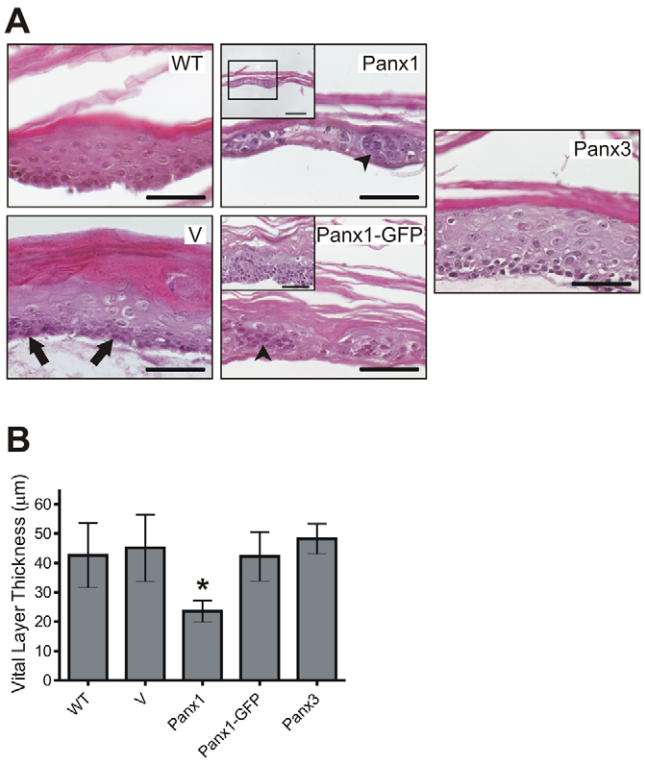

Fig. 9. Overexpression of Panx1 disrupted the architecture of the epidermis and decreased the vital layer thickness. (**A**) H&E-stained images of organotypic epidermis revealed similar differentiation profiles between wild-type (WT), vector (V) and Panx3-overexpressing organotypic cultures. Nuclei of undifferentiated keratinocytes appeared dark pink (arrows), whereas the basophilic cornified layer was stained bright pink. By contrast, Panx1 and Panx1-GFP revealed differentiation phenotypes that were dysregulated, as indicated by the pockets of undifferentiated-appearing keratinocytes (arrowheads). Vital layer thickness of Panx1-GFP cultures revealed both thin and thick phenotypes (inserts). (**B**) In addition to the dysregulated phenotype, Panx1-overexpressing organotypic epidermis revealed that the vital layer thickness was reduced. Asterisks denote statistical significance (n=5, P<0.05) and bar graphs show means ± s.d.

Discussion

Almost a decade after their discovery in the mammalian genome (Panchin et al., 2000), pannexins have been classified as single-membrane channels with a broad range of tissue-expression patterns, including the skin (Penuela et al., 2007; Scemes et al., 2009). Although the debate on whether pannexins form only single-membrane channels continues, the diverse expression profiles of Panx1 and Panx3 observed in several cell and tissue types highlight the complexity of their possible cellular roles. Thus, we hypothesized that Panx1 and Panx3 play key roles in epidermal keratinocyte differentiation. In this study, we demonstrate that keratinocyte differentiation was dysregulated upon ectopic Panx1 expression, but not Panx3, suggesting that these pannexins play diverse roles when coexpressed in the same tissue.

Differential Panx1 and Panx3 protein expression in murine skin

To begin to understand the putative roles of Panx1 and Panx3 in murine skin, the differential distribution profiles of these pannexins

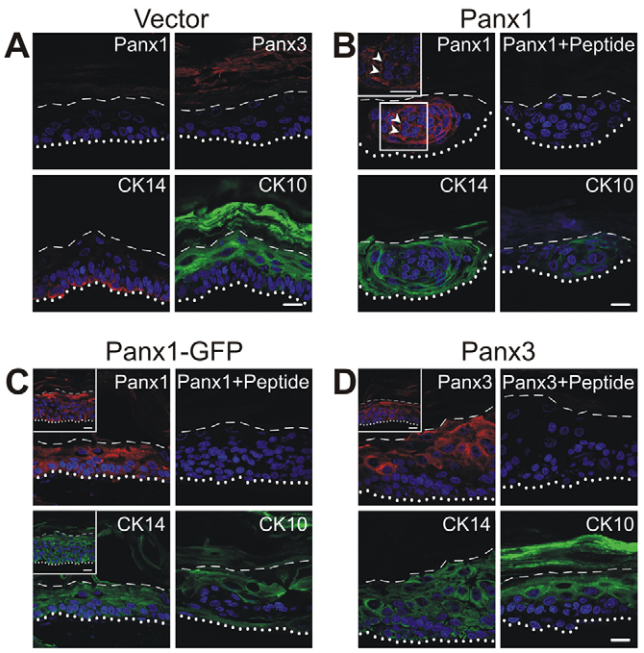

Fig. 10. Exogenous Panx1 and Panx3 differentially affect the differentiation of the epidermis, as exhibited by the localization of CK14 and CK10. (**A**) Immunofluorescent images of organotypic epidermis grown from empty-vector-expressing REKs revealed the detection of Panx3 (red) in the cornified layer, whereas Panx1 expression was below detectable levels in the vital layer. As expected, CK14 (red) was mainly localized to the basal layer, whereas CK10 (green) was found in suprabasal layers of control epidermis. (**B**) When Panx1 was ectopically expressed, it was localized throughout the epidermis in intracellular compartments and occasionally at the cell surface (arrowheads). CK14 expression was detected in irregular patterns and the cells exhibited weak CK10 expression in both Panx1- (B) and Panx1-GFP- (**C**) expressing cells. (**D**) In cells engineered to overexpress Panx3, Panx3 and CK14 were found throughout all epidermal layers, whereas CK10 was localized only to suprabasal layers. The basal layer is denoted above the dotted line and the cornified layer is located above the dashed lines. Hoechst nuclear stain is shown in blue. Scale bars: 20 µm.

were assessed. Early in embryonic development, both Panx1 and Panx3 were easily detected in the epidermis of E13.5 embryos. After birth, Panx1 was detected in all epidermal layers of thin epidermis, but was only found in the suprabasal layer of newborn epidermis. Although predominately punctate Panx1 staining was detected in human facial epidermis (Penuela et al., 2007), we observed a diffuse intracellular expression profile of Panx1 in murine epidermis, suggesting that Panx1 localization might vary among animal species. On the other hand, the diffuse intracellular Panx3 staining observed throughout all epidermal layers in the murine epidermis was consistent with that of human facial epidermis (Penuela et al., 2007). Moreover, western blots revealed glycosylated Panx3 species at ~43 kDa and a second immunoreactive species at ~70 kDa. Interestingly, intense Panx3 staining was revealed in sebocytes, raising the possibility that Panx3 might be involved in sebocyte function or regulation.

Panx1 and Panx3 have already been implicated in cellular communication with the extracellular environment through single-membrane channels (Locovei et al., 2006; Penuela et al., 2007). However, the diffuse intracellular localization profiles revealed in the murine epidermis suggest that they could have a second function that might be tissue and species specific. In fact, Vanden Abeele et al. suggested that Panx1 might regulate intracellular calcium homeostasis through ER calcium leak channels (Vanden Abeele et al., 2006). Of further note, the decreased expression of Panx1 in thin and thick skin compared with that in newborn skin suggests that Panx1 might play an important role early in skin generation, but be of less importance in skin maintenance. This concept is not without precedence, as the cytokeratin composition changes in aged and dry epidermis, exemplifying the adaptation of skin to changes in the external environment (Engelke et al., 1997). Thus, the spatio-temporal regulation of Panx1 and Panx3, and their differential subcellular localization patterns suggest that these pannexins might play distinct roles within the epidermis.

Characterization of exogenously expressed Panx1, Panx1-GFP and Panx3 in REKs

Because REKs possess the ability to differentiate into organotypic epidermis and express low levels of endogenous Panx1 and Panx3, they represent an excellent model to investigate the cellular role of pannexins. As might be expected, overexpressed Panx1, Panx1-GFP and Panx3 localized predominantly to the cell surface in the majority of REKs when cultured in monolayer, supporting the premise that the major function of these pannexins occurs at the cell surface, presumably through communication with the extracellular environment. REKs that expressed Panx1, Panx1-GFP or Panx3 were indeed competent for dye uptake upon mechanical stimulation, suggesting the presence of functional cell-surface channels. These findings are consistent with the cell-surface localization of ectopic Panx1 and Panx3 in REK, Madin-Darby canine kidney and gap-junction-deficient HeLa cells, as well as the formation of channels capable of dye uptake when 293T cells expressed Panx1 or Panx3 (Penuela et al., 2007; Penuela et al., 2009; Penuela et al., 2008). In a variety of cell types, cell-surface Panx1 channels were found to pass electrical current and dyes, as well as release ATP (Bruzzone et al., 2005; Penuela et al., 2007; Ransford et al., 2009). Intriguingly, Panx3 revealed a second distinct intracellular distribution pattern not unlike that found in human skin keratinocytes, mouse spleen lymphocytes, mouse osteoblasts and some rat neuroblastoma cells (Penuela et al., 2007; Penuela et al., 2008). The reason for this distribution pattern is not clear, but might reflect changes in the differentiation status of individual keratinocytes. This suggestion is supported by the fact that Panx3 was found almost exclusively in intracellular compartments when Panx3-expressing REKs were grown into organotypic epidermis. Interestingly, ectopic Panx1 also acquired a predominantly intracellular distribution when keratinocytes were grown as organotypic epidermis, further suggesting that the differentiation program promotes keratinocytes to relocalize Panx1 and Panx3.

One emerging role of Panx1 and Panx3 at the cellular level might involve the regulation of cell proliferation. On the basis of BrdU incorporation, Panx1 and Panx3 decreased keratinocyte proliferation, which is consistent with the Panx1-induced decrease in the proliferation of C6 gliomas (Lai et al., 2007). It is possible that the even small changes in the rate of cellular proliferation might have larger disruptive effects on the delicate balance between cell proliferation and cell differentiation. However, this is not likely to be the case here, as Panx3 also caused a decrease in proliferation; however, the ability of REKs to differentiate, as assessed by the architecture of the tissue and the markers of differentiation, remained relatively unchanged.

Panx1 dysregulates keratinocyte differentiation, whereas Panx3 maintains epidermal architecture

Using our model of keratinocyte differentiation, we revealed that ectopic Panx1, Panx1-GFP and Panx3 predominantly redistributed from the cell surface to intracellular compartments. This, in fact, more accurately reflects the distribution profile of endogenous Panx1 and Panx3 in mouse skin. However, several lines of evidence suggest that Panx1 overexpression dysregulates keratinocyte differentiation. First, the expression level of CK14, a common marker of undifferentiated basal keratinocytes, was increased throughout all vital layers in the organotypic epidermis compared with monolayer REKs. Second, the architecture of the organotypic epidermis was highly disorganized. Third, there was a reduction in the vital layer thickness. Finally, the localization of CK10 was abnormal. Taken together with the in vivo finding that Panx1 is reduced in aged skin compared with newborn skin, Panx1 might be more important in epidermal development and generation than in maintenance and renewal. In essence, it is possible that Panx1 expression might delay the differentiation of keratinocytes in newly forming epidermis, only to be downregulated when keratinocytes signal to increase differentiation. Although GFP-tagged Panx1 displayed a dysregulated epidermal architecture similar to that of untagged Panx1, the response appeared attenuated because the vital layer thickness and CK14 levels remained similar to those of the control. This might be explained in part by the fact that, in one report, it was shown that the GFP tag reduced Panx1 channel function (Ma et al., 2009).

In contrast to Panx1, Panx3 expression did not alter the integrity of the organotypic epidermis, and both our in vivo and in vitro evidence further suggests that Panx3 might in fact support keratinocyte differentiation. Differentiation of REKs into organotypic epidermis increased the expression level of the 70 kDa immunoreactive species of endogenous Panx3. The localization of this unique species of Panx3 remains unclear, but it was notable that the cornified layer of wild-type organotypic epidermis was specifically stained with anti-Panx3 antibodies. One possibility is that the ~70 kDa immunoreactive species of Panx3 is associated with programmed cell death, as the keratinocytes fully differentiate and form the dead cornified layer. This possibility is not without precedent, as the classic differentiation markers CK10 and involucrin are known to have increased expression levels in differentiating keratinocytes and even localize to the cornified layer (Chen et al., 2006; Hara-Chikuma et al., 2009). Further support for the role of Panx3 in epidermal maintenance is the finding that the integrity of the organotypic epidermis did not appear dysregulated when the ~43 kDa species of Panx3 was overexpressed. Similar to endogenous Panx3 in human facial skin (Penuela et al., 2007), Panx3 primarily localizes to an intracellular compartment that is probably the site of its function in differentiated keratinocytes.

In summary, our two- and three-dimensional in vitro studies support the hypothesis that Panx1 and Panx3 play key and distinct roles in keratinocyte differentiation and proliferation. This study revealed that Panx1 must be exquisitely regulated to enable new epidermis formation and to maintain a healthy epidermis. Furthermore, our studies suggest that Panx1 and Panx3 acquire distinct subcellular localizations depending on the state of keratinocyte differentiation. Future research should be directed towards investigating how pannexin single-membrane channels fulfill their roles in keratinocyte differentiation and proliferation both at the cell surface and within intracellular compartments.

Materials and Methods

Generation of Panx1, Panx1-GFP and Panx3 stable cell lines

All cell-culture reagents were obtained from Invitrogen and Becton-Dickinson (BD). REK cell lines were cultured in Dulbecco's modified essential medium (DMEM) supplemented with 10% FBS, 100 U/ml penicillin, 100 μg/ml streptomycin and 2 mM L-glutamine in a humid environment at 37°C and 5.0% CO_2 as described (Maher et al., 2005). REK cell lines were engineered to express an empty vector (V), Panx1, GFP-tagged Panx1 (Panx1-GFP) or Panx3 using sequence-validated cDNA constructs (Penuela et al., 2007) incorporated into AP2-replication-defective retroviral vectors as described (Galipeau, 1999; Qin et al., 2002). Infection protocols were performed serially three times as described (Mao et al., 2000). Briefly, OptiMEM medium containing Lipofectamine2000 was used to transfect each of the constructs into the 293GPG packaging cell line to produce replication-defective virus-containing supernatant. Supernatants were filtered through 0.45 mm filters, then incubated on low-density plated wild-type (WT) REKs in 35 mm dishes at 37°C as previously described (Mao et al., 2000; Thomas et al., 2007). Up to passage 4, pannexin expression was 85-95% efficient, as determined by immunofluorescent labeling of pannexins and assessing the percentage of cells (n>2000 cells) expressing pannexins compared with cells positive for the Hoechst 33342 nuclear stain (data not shown). For all experiments, passage 2-4 cells were used.

Organotypic epidermis as a model of keratinocyte differentiation

REK cell lines were used to grow organotypic epidermis as described (Maher et al., 2005; Thomas et al., 2007). Briefly, 5×10^5 cells were plated on 24 mm transwell filter inserts containing 3 μm pores (BD Labware) coated with 1 ml type I rat tail collagen (BD Biosciences) and bathed in REK growth medium above and below the filter. When the cells grew to confluence after 3 days, the top media was removed, exposing the REKs to air. Air exposure stimulated the differentiation and stratification of each REK cell line, and these cultures were maintained for 21 days after air exposure. In addition, REK growth media was changed daily.

Dissection of murine skin

Mouse skin was handled in accordance with the standard operating procedures outlined by the University of Western Ontario and the International Guide for the Care and Use of Laboratory Animals published by the United States National Institutes of Health (NIH publication number 85-23, revised 1996). To identify the localization of Panx1 and Panx3 in skin, 1 cm^2 biopsies were obtained from newborn and 21-day-old (adult) C57/BL6 mice. Specifically, the trunk portion of newborn and shaved dorsal (thin) and paw (thick) adult skin was collected, and subsequently used for histochemical and western blot analysis.

Immunolabeling

To study the localization of Panx1 and Panx3 at the cellular level in keratinocytes, REKs were grown on coverslips and immunolabeled as previously described (Thomas et al., 2007), with some modifications. Briefly, cells were fixed in an 80% methanol-20% acetone solution for 20 minutes at 4°C and blocked with 3% BSA (Sigma-Aldrich) in PBS at room temperature for 45 minutes. Cells were incubated with 2 μg/ml anti-Panx1 or anti-Panx3 affinity-purified primary antibodies [generated and described in Penuela et al. (Penuela et al., 2007)], PDI (1:500; Stressgen) or the anti-G3G4 antibody directed against BrdU (1:100; Developmental Studies Hybridoma Bank) primary antibody for 1 hour at room temperature. Cells were then incubated with secondary antibodies AlexaFluor555, AlexaFluor488 (1:500; Invitrogen) or Texas Red (1:200; Jackson ImmunoResearch) for 1 hour at room temperature, followed by counterstaining with 10 μg/ml Hoechst 33342 to denote nuclei, and mounted. As a negative control, peptide pre-adsorption assays were performed as described in Penuela et al. (Penuela et al., 2007) to account for any non-specific staining. All immunolabeling experiments were analyzed using a Zeiss LSM 510 META inverted confocal microscope system as described in Thomas et al. (Thomas et al., 2007), except that a 63× oil objective lens was used to assess the localization patterns. Each experimental group was imaged under identical instrument-configuration settings.

In other studies, E13.5 mice were embedded into paraffin and cut into 5 μm sections. Sections were double labeled with either anti-Panx1 (20 μg/ml) or anti-Panx3 (20 μg/ml) antibodies, in addition to an anti-cytokeratin 14 antibody (1:250; Neomarkers). As controls, specific anti-pannexin labeling was competed with cognate peptides at a 50:1 molar ratio of peptide to antibody, whereas the primary antibody was eliminated for CK14 labeling. All sections were then incubated with anti-rabbit AlexaFluor555 and anti-mouse AlexaFluor488 (Molecular Probes) for 1 hour at room temperature, washed and imaged as described above.

Dye uptake experiments

Stable REK cell lines expressing Panx1, Panx1-GFP, Panx3 or the empty vector were plated in 35 mm culture dishes coated with 0.5 mg/ml collagen type I in 60% ethanol. All cultures were kept on ice and subjected to sulforhodamine B (molecular weight 559, Invitrogen) dye-uptake assays under conditions of physiological Ca^{2+} and Mg^{2+} and mechanical stimulation, as we described in detail earlier (Penuela et al., 2007; Penuela et al., 2009). Briefly, cell cultures were rinsed twice with ice-cold D-PBS and mechanically stimulated with a continuous drip of 800 μl of dye released from a height 2.5 cm above the culture dish. The drip was repeated three times and the dye-covered cells were set on ice for 5 minutes. After several washes with cold D-

PBS, the dishes were examined under a Leica microsystems fluorescent microscope equipped with a Hamamatsu digital camera and Openlab software. Experiments were repeated two additional times with separate populations of cells, yielding similar results. Dextran-rhodamine (molecular weight 10,000; Invitrogen) was used in parallel as a negative control.

REK proliferation assay

To assess the proliferation status of our engineered REK cell lines, 2×10^4 cells were seeded on coverslips in 35 mm dishes for 24 hours and subsequently incubated with 10 μM BrdU (Sigma-Aldrich) for 4 hours at 37°C. Cells were processed for immunocytochemistry as described above, except that DNA was denatured using 2 M HCl for 20 minutes at room temperature following fixation. At least 2000 cells per cell line (n=5) were counted, and the percentage of BrdU-positive staining nuclei versus total nuclei denoted by Hoechst 33342 staining was assessed.

REK migration assay

The migration capabilities of REK cell lines were assessed using a scrape assay as described by Thomas et al. (Thomas et al., 2007), with the following modifications. Cells were plated at a concentration of 2×10^5 on 35 mm dishes that contained a calibrated grid. After 36 hours, cells were confluent and a 16 cm rubber cell scraper (Sarstedt) was used to carefully scrape cells off the center of the dish. Cells were allowed to migrate in OptiMEM medium for 48 hours, then fixed with 3.7% formaldehyde for 30 minutes at room temperature and viewed using a Leica microscope. At least 50 images per cell line (n=5) that displayed clear cell migration were blindly selected, measured in three predetermined locations using Adobe Photoshop CS2 software and averaged.

Organotypic epidermis and murine skin histochemistry

To determine the architecture and localization of Panx1 and Panx3 in organotypic epidermis and murine skin, samples were preserved and processed as previously described in Thomas et al. (Thomas et al., 2007), with some modifications. Approximately 1 cm^2 samples were preserved in 10% neutral buffered formalin overnight at 4°C. Samples were dehydrated in a graded series of ethanol and then xylene, and embedded in paraffin wax. Using the Leica RM2125RT microtome (Leica Microsystems), 5-7 μm sections were prepared on glass slides. Slides were independently stained with Harris H&E for 5 minutes each and mounted with Cytoseal (Canadawide Scientific) to reveal the epidermal architecture. Stained sections were subsequently viewed with an AxioPlan2 microscope (Carl Zeiss) equipped with a 63× lens and imaged using an AxioCam camera with AxioVision LE Rel. 4.3 imaging software (Carl Zeiss).

To assess the differentiation capabilities of pannexin-overexpressing cell lines, the vital layer thickness was measured using H&E-stained organotypic epidermis and the Axiovision software. Three measurements, at predetermined locations (60, 120 and 180 μm along the x-axis ruler), were taken per image at right angles from the bottom of the basal layer to the top of the suprabasal layer and averaged. At least 50 images were used per cell line collected from at least five epidermal preparations.

Immunohistochemistry of tissue samples was also used to examine the localization of Panx1 and Panx3, as described by Penuela et al. (Penuela et al., 2007) with some modifications. Briefly, antigen retrieval was performed on all slides using 0.01 M sodium citrate buffer, pH 6.0 and microwaved for 2.5 minutes at 80% power. Non-specific labeling was blocked with 3% BSA and 0.1% Triton-X-100 (Sigma-Aldrich) for 45 minutes at room temperature. Affinity-purified anti-Panx1 and anti-Panx3 antibodies (4 μg/ml; Penuela et al., 2007), as well as anti-CK14 (1:100; Neomarkers) or anti-CK10 (1:100; Neomarkers) primary antibodies were incubated at 4°C overnight. Samples were incubated with secondary antibodies AlexaFluor555 or AlexaFluor488 (1:500; Invitrogen) for 1 hour at room temperature and counterstained with 10 μg/ml Hoechst 33342 to denote nuclei prior to mounting with Vectashield (Vector Laboratories). As a control, peptide pre-adsorption assays were used in parallel as described above. Analysis was performed using the Zeiss LSM 510 META inverted confocal microscope system.

Immunoblotting

To determine the levels of Panx1 and Panx3 expression, lysates were extracted from cell lines, organotypic epidermis and murine skin using a Triton-based extraction buffer as described by Penuela et al. (Penuela et al., 2007). Protein was quantified using a bicinchonic acid assay (Pierce). Samples (25 μg of cell lysates and 35 μg of tissue lysates) were boiled for 10 minutes, separated using 10% SDS-PAGE and then transferred to a nitrocellulose membrane. Membranes were blocked with 5% Blotto, non-fat dry milk (Santa Cruz Biotechnology) and 0.05% Tween20 in PBS for 30 minutes at room temperature. Affinity-purified anti-Panx1 or anti-Panx3 antibody (0.4 μg/ml; Penuela et al., 2007), as well as anti-CK14 (1:1000; Neomarkers) or anti-involucrin (1:1000; Covance Research Products) primary antibodies were incubated at 4°C overnight. Anti-GAPDH antibodies (1:20000; Chemicon/Millipore) were used to assess equal loading. Following washes with PBS-Tween20, either AlexaFluor680 (1:5000; Invitrogen) or IRDye800 (1:5000; Rockland) secondary antibodies were used, and membranes were visualized with an Odyssey infrared imaging system (LiCor). As a control, peptide pre-adsorption assays were used as described earlier. The densitometry of unsaturated images was analyzed using Odyssey 2.0.4 application software (LiCor). Quantified protein levels were normalized to GAPDH and expressed relative to control samples (newborn skin or monolayer wild-type REKs). Western blot results were averaged for at least three mouse skin experiments and five monolayer or organotypic epidermis culture experiments.

Statistical analysis

For all quantified experiments, the raw data were subjected to a one-way analysis of variance (ANOVA) to determine whether significant differences existed between the experimental groups. For the proliferation, migration and vital layer measurements, a Tukey's multiple comparison post-hoc test was used to indicate whether significant differences existed between any of the groups (P<0.05). Western blot analysis was coupled to the Dunnett's multiple comparison post-hoc test (P<0.05). All tests were performed and displayed using GraphPad Prism 4.03 software.

D.W.L., K.N.C. and S.J.C. are supported by the Canadian Institutes of Health Research, the London Regional Cancer Program, or the National Sciences and Engineering Research Council of Canada.

References

Bao, L., Locovei, S. and Dahl, G. (2004). Pannexin membrane channels are mechanosensitive conduits for ATP. *FEBS Lett.* **572**, 65-68.

Baranova, A., Ivanov, D., Petrash, N., Pestova, A., Skoblov, M., Kelmanson, I., Shagin, D., Nazarenko, S., Geraymovych, E., Litvin, O. et al. (2004). The mammalian pannexin family is homologous to the invertebrate innexin gap junction proteins. *Genomics* **83**, 706-716.

Boassa, D., Ambrosi, C., Qiu, F., Dahl, G., Gaietta, G. and Sosinsky, G. (2007). Pannexin1 channels contain a glycosylation site that targets the hexamer to the plasma membrane. *J. Biol. Chem.* **282**, 31733-31743.

Bruzzone, R., Barbe, M. T., Jakob, N. J. and Monyer, H. (2005). Pharmacological properties of homomeric and heteromeric pannexin hemichannels expressed in Xenopus oocytes. *J. Neurochem.* **92**, 1033-1043.

Chen, J., Cheng, X., Merched-Sauvage, M., Caulin, C., Roop, D. R. and Koch, P. J. (2006). An unexpected role for keratin 10 end domains in susceptibility to skin cancer. *J. Cell Sci.* **119**, 5067-5076.

Engelke, M., Jensen, J. M., Ekanayake-Mudiyanselage, S. and Proksch, E. (1997). Effects of xerosis and ageing on epidermal proliferation and differentiation. *Br. J. Dermatol.* **137**, 219-225.

Galipeau, J. L. H., Paquin, A., Sicilia, F., Karpati, G. and Nalbantoglu, J. (1999). Vesicular Stomatis Virus G pseudotyped retrovector mediates effective in vivo suicide gene delivery in experimental brain cancer. *Cancer Res.* **59**, 2384-2394.

Hara-Chikuma, M., Takahashi, K., Chikuma, S., Verkman, A. S. and Miyachi, Y. (2009). The expression of differentiation markers in aquaporin-3 deficient epidermis. *Arch. Dermatol. Res.* **301**, 245-252.

Iglesias, R., Dahl, G., Qiu, F., Spray, D. C. and Scemes, E. (2009). Pannexin 1, the molecular substrate of astrocyte "hemichannels". *J. Neurosci.* **29**, 7092-7097.

Lai, C. P., Bechberger, J. F., Thompson, R. J., MacVicar, B. A., Bruzzone, R. and Naus, C. C. (2007). Tumor-suppressive effects of pannexin 1 in C6 glioma cells. *Cancer Res.* **67**, 1545-1554.

Langlois, S., Maher, A. C., Manias, J. L., Shao, Q., Kidder, G. M. and Laird, D. W. (2007). Connexin levels regulate keratinocyte differentiation in the epidermis. *J. Biol. Chem.* **282**, 30171-30180.

Locovei, S., Wang, J. and Dahl, G. (2006). Activation of pannexin 1 channels by ATP through P2Y receptors and by cytoplasmic calcium. *FEBS Lett.* **580**, 239-244.

Ma, W., Hui, H., Pelegrin, P. and Surprenant, A. (2009). Pharmacological characterization of pannexin-1 currents expressed in mammalian cells. *J. Pharmacol. Exp. Ther.* **328**, 409-418.

Maher, A. C., Thomas, T., Riley, J. L., Veitch, G., Shao, Q. and Laird, D. W. (2005). Rat epidermal keratinocytes as an organotypic model for examining the role of Cx43 and Cx26 in skin differentiation. *Cell Commun. Adhes.* **12**, 219-230.

Mao, A. J., Bechberger, J., Lidington, D., Galipeau, J., Laird, D. W. and Naus, C. C. (2000). Neuronal differentiation and growth control of neuro-2a cells after retroviral gene delivery of connexin43. *J. Biol. Chem.* **275**, 34407-34414.

Panchin, Y., Kelmanson, I., Matz, M., Lukyanov, K., Usman, N. and Lukyanov, S. (2000). A ubiquitous family of putative gap junction molecules. *Curr. Biol.* **10**, R473-R474.

Penuela, S., Bhalla, R., Gong, X. Q., Cowan, K. N., Celetti, S. J., Cowan, B. J., Bai, D., Shao, Q. and Laird, D. W. (2007). Pannexin 1 and pannexin 3 are glycoproteins that exhibit many distinct characteristics from the connexin family of gap junction proteins. *J. Cell Sci.* **120**, 3772-3783.

Penuela, S., Celetti, S. J., Bhalla, R., Shao, Q. and Laird, D. W. (2008). Diverse subcellular distribution profiles of pannexin 1 and pannexin 3. *Cell Commun. Adhes.* **15**, 133-142.

Penuela, S., Bhalla, R., Nag, K. and Laird, D. W. (2009). Glycosylation regulates pannexin intermixing and cellular localization. *Mol. Biol. Cell* **20**, 4313-4323.

Qin, H., Shao, Q., Curtis, H., Galipeau, J., Belliveau, D. J., Wang, T., Alaoui-Jamali, M. A. and Laird, D. W. (2002). Retroviral delivery of connexin genes to human breast tumor cells inhibits in vivo tumor growth by a mechanism that is independent of significant gap junctional intercellular communication. *J. Biol. Chem.* **277**, 29132-29138.

Ransford, G. A., Fregien, N., Qiu, F., Dahl, G., Conner, G. E. and Salathe, M. (2009). Pannexin 1 contributes to ATP release in airway epithelia. *Am. J. Respir. Cell Mol. Biol.* **41**, 525-534.

Scemes, E., Spray, D. C. and Meda, P. (2009). Connexins, pannexins, innexins: novel roles of "hemi-channels". *Pflugers Arch.* **457**, 1207-1226.

Silverman, W. R., de Rivero Vaccari, J. P., Locovei, S., Qiu, F., Carlsson, S. K., Scemes, E., Keane, R. W. and Dahl, G. (2009). The pannexin 1 channel activates the inflammasome in neurons and astrocytes. *J. Biol. Chem.* **284**, 18143-18151.

Thomas, T., Shao, Q. and Laird, D. W. (2007). Differentiation of organotypic epidermis in the presence of skin disease-linked dominant-negative Cx26 mutants and knockdown Cx26. *J. Membr. Biol.* **217**, 93-104.

Vanden Abeele, F., Bidaux, G., Gordienko, D., Beck, B., Panchin, Y. V., Baranova, A. V., Ivanov, D. V., Skryma, R. and Prevarskaya, N. (2006). Functional implications of calcium permeability of the channel formed by pannexin 1. *J. Cell Biol.* **174**, 535-546.

Zoidl, G., Petrasch-Parwez, E., Ray, A., Meier, C., Bunse, S., Habbes, H. W., Dahl, G. and Dermietzel, R. (2007). Localization of the pannexin1 protein at postsynaptic sites in the cerebral cortex and hippocampus. *Neuroscience* **146**, 9-16.